

## Enhancing Pullout Capacity of Single Piles and Pile Groups Using Geosynthetic Soil-Reinforcement Technique

Asmaa Nour El-Deen<sup>1,\*</sup>, Marawan Shahien<sup>2</sup>, Mona Mansour<sup>3</sup>, Mohamed Rabie<sup>4</sup>

<sup>1</sup> Ph.D. Candidate, Assistant Lecturer, Faculty of Engineering, Helwan University, Mataria branch, Cairo, Egypt

<sup>2</sup> Prof. of Geotechnical Engineering, Civil Engineering Department, Faculty of Engineering, Tanta University, Cairo, Egypt

<sup>3</sup> Prof. of Geotechnical Engineering, Civil Engineering Department Faculty of Engineering, Helwan University, Mataria branch, Cairo, Egypt

<sup>4</sup> Prof. of Geotechnical Engineering, Civil Engineering Department, Faculty of Engineering, Helwan University, Mataria branch, Cairo, Egypt

\*Corresponding author E-mail: [asmaa\\_noreldein@m-eng.helwan.edu.eg](mailto:asmaa_noreldein@m-eng.helwan.edu.eg)

**Abstract.** This study investigates the influence of soil reinforcement on the uplift performance of single piles and pile groups in cohesionless soil with 60% relative density. Various reinforcement configurations were examined, altering reinforcement type, embedded depth, layer width, and number of layers. Steel circular piles with bulged surfaces were used for the single pile and the 2x1 pile group models, with the latter spaced at three times the single pile diameter. Results demonstrate that the incorporation of soil reinforcement layers significantly improved the pullout capacity of the single pile and the 2x1 pile group. In addition, the pullout resistance increases with reinforcement layer width, up to 9D for single piles and (9+3) D for pile groups, where D is the diameter of the single pile. Multiple reinforcement layers further enhanced pullout resistance for both configurations. For pile groups, a double layer of geogrid spaced at 2D yielded superior pile capacity ratios compared to a single layer, though single-layer configurations exhibited higher group efficiency. The study also compares the effects of two reinforcement types, SS30 and TX150, on pullout capacity. Numerical simulations using Abaqus software complement the experimental findings, validating the observed enhanced pullout capacities in reinforced soil conditions. This research contributes valuable insights into optimizing pile foundation design through strategic soil reinforcement techniques, potentially revolutionizing geotechnical engineering practices for enhanced structural stability and cost-effectiveness.

**Keywords:** Soil reinforcement, Pile group, Pullout load, SS30, TX150.

## 1. INTRODUCTION

Several constructions require more advanced, complicated, and deep foundations due to the magnitude of the loads that affect and the depth of the strong soil layers that can carry such loads. Pile foundations became the main solution approach for these types of structures several years ago. Piles utilized in various fields of engineering, for example retaining walls, high-rise

buildings, offshore platforms, slope stability, quay walls, and wind turbine foundations, are subjected to significant uplift forces generated by eccentric loading, wind action, and upward-acting forces ([1]; [2]; [3]; [4]; [5]).

Furthermore, these foundations are subjected to horizontal forces and bending moments induced by lateral earth pressures, wave action, and seismic loads. The design of pile foundations experiencing such loading conditions can incorporate various configurations and dimensions. Depending on project requirements, these foundation systems may be implemented either as a single pile or as a pile group. As the area influenced by the piles contributes a significant role in the behavior of the piles, pile groups exhibit more distinct behavior than a single pile. Single pile uplift resistance is primarily derived from the pile's self-weight, shaft friction, and the mass of soil mobilized within the failure mechanism. The required capacity can be achieved through modifications to the pile surface area, embedment depth ratio, and soil density parameters. On the other hand, for pile groups, optimal performance is attained through careful selection of the spacing ratio between the piles. So, comprehending pile performance and accurately estimating pile capacity when subjected to uplift forces are crucial aspects in the design of robust and efficient foundations.

While, geosynthetic materials have gained widespread adoption in various geotechnical engineering applications, including stabilization of embankments on soft soils, construction of road layers, and foundation systems, as evidenced by numerous studies (e.g., [6]; [7]; [8]; [9]; [10]; [11]; [12]; [13]; [14]). However, the behavior of piles in reinforced soil under uplift loading conditions has gained insufficient research attention ([15]; [16]; [17]; [18], [19]), highlighting a significant gap in our understanding of these critical foundation elements.

K. Ilamparuthi and E. A. Dickin [19] conducted a comprehensive study on the impact of geogrid soil reinforcement on the behavior of uplift scaled-down belled piles in sandy soil. Their findings revealed that several factors contribute to enhanced pull-out resistance: an increase in geogrid cell diameter, higher density of the sand, larger the bell diameter, and greater embedment depth. This research elucidated the complex interplay between soil reinforcement and pile geometry in determining uplift capacity, providing valuable insights for optimizing foundation design in reinforced soil conditions.

In their study, A. Ghosh and A. K. Bera [17] examined experimentally how geotextile reinforcement influences the uplift resistance of embedded sand anchors and enlarged pile bases. Their findings demonstrated that uplift capacity increases proportionally with both the embedment depth-to-base diameter ratio and the number of geotextile layers. The optimal number of reinforcement layers for tying was determined approximately as 2.4 times the pile diameter.

S. V. K. Rao and A. M. Nasr [20] examined the performance of vertical individual piles that were installed into cohesionless soil, both with and without reinforcement, using small-scale model experiments. Their experimental program utilized three circular reinforced concrete piles with distinct surface textures for pullout testing. An investigation was carried out to examine the effect of geogrid sand reinforcing on the uplift behavior of model piles. Parameters investigated included pullout load orientation, reinforcement depth, number of reinforcing layers, and the length of each layer. Experimental outcomes demonstrated that pullout resistance correlates positively with concrete surface roughness, sand density, and reinforcement incorporation. Furthermore, their findings established that reinforcement effectiveness is significantly influenced by the concrete surface texture characteristics.

B. Li and J. Fu [21] reported that the major approach for assessing the uplift capacity of piles in soil foundations is through load testing, which is both time-consuming and inefficient. The pile-soil interface friction is simulated using a small sliding model and contact pairs in the ABAQUS finite element program. This simulation results in a well-fitted curve for the pile foundation capacity assessment. Based on the findings from the finite element software, the lateral friction of the pile has reached its maximum capacity, and the stress on the pile increases steadily as the pile displacement increases, until it reaches its maximum pullout capacity. The ABAQUS software is able to simulate the uplift capacity of piles.

J. Jiang, Z. Mao, L. Chen, and Y. Wu [22] conducted a study that investigated the impact of several important parameters on uplift pile capacity, including pile diameter, composite-anchor cable quantity, and steel strand dimensions. Their investigation employed a validated three-dimensional finite element analysis using ABAQUS 2020, with the computational model being calibrated against field measurements.

Previous work has mostly focused on the piles load-displacement characteristics in two instances: unreinforced foundations and foundations reinforced with horizontal reinforcement such as geotextiles and geogrids, specifically when subjected to static uplift loads. Hence, the literature described above highlights a significant lack of research on the behavior of the piles under pull-out forces which are embedded in reinforced soil.

Comprehensive laboratory investigations were performed to enhance understanding of pullout response in both single piles and pile groups buried in reinforced soil. The research methodology incorporated validated three-dimensional finite element analysis, against experimental data from both reinforced and unreinforced soil conditions. The investigation primarily focused on showcase the advantages of reinforcement, specifically by comparing the uplift behaviour of single piles and pile groups in geogrid-reinforced and geogrid-unreinforced systems.

## 2. EXPERIMENTAL ANALYSIS

### 2.1. Material Properties

In our experimental investigation, we conducted pullout tests on both single piles and pile groups reinforced by two types of geogrid (SS30) and (TX150). The single pile configuration consisted of a circular steel pile featuring bulges, connected to a square footing plate serving as the pile cap for the structural assembly. For the pile group tests, we employed a (2x1) arrangement with an inter-pile spacing of three times the single pile diameter.

Our experimental design was informed by [23] recommendation that the optimal height-to-diameter ratio for the model pile is 10:1. Therefore, we dimensioned our model piles to be 35 mm in diameter and 350 mm in length. The footing plate was a 3 mm thick rigid steel plate. The experimental setups for the single pile and pile group configurations are illustrated in Fig.1 and Fig. 2, respectively. These schematic representations provide a clear visual depiction of the test arrangements, facilitating a comprehensive understanding of the experimental methodology.



**Fig.1** The model of the circular steel pile with bulges used in the present study.

In the current investigation, we focused on sandy soils commonly utilized in construction-related compaction work to examine the effects of the reinforced soil on the performance of both single vertical piles and pile groups subjected to pullout forces. Our laboratory program encompassed sieve analysis, modified proctor compaction, and direct shear tests on the sandy soil specimens. Table 1 displays a comprehensive brief of the soil's features, including its composition, classification, maximum dry densities, and optimum moisture contents. Furthermore, we report the minimum dry densities, as well as the curvature and uniformity coefficients.

**Table 1** Properties of the tested soil

<i>Parameter</i>	<i>Symbol and unit</i>	<i>Value</i>
<i>Maximum dry unit weight</i>	$\gamma_{dmax}$ (t/m <sup>3</sup> )	1.93
<i>Minimum dry unit weight</i>	$\gamma_{dmin}$ (t/m <sup>3</sup> )	1.72
<i>Maximum void ratio</i>	$e_{max}$	0.52
<i>Minimum void ratio</i>	$e_{min}$	0.36
<i>Specific gravity</i>	G <sub>s</sub>	2.62
<i>Gravel</i>	%	13.6
<i>Coarse sand</i>	%	52.9
<i>Medium sand</i>	%	33.3
<i>Fine sand</i>	%	0.21
<i>Effective grain size</i>	D <sub>10</sub> (mm)	0.34
<i>Uniformity coefficient</i>	C <sub>u</sub>	3.53
<i>Coefficient of curvature</i>	C <sub>c</sub>	0.74
<i>Classification</i>	Sp	-
<i>Optimum moisture content</i>	O.M.C (%)	5.8
<i>Relative density</i>	%	60
<i>Dry unit weight</i>	$\gamma_d$ (t/m <sup>3</sup> )	1.84
<i>Water content</i>	w.c (%)	4



**Fig. 2** The model of the (2x1) pile group.

## 2.2. Model preparation and pile installation

For our experimental program, we utilized a custom-designed metal container with dimensions of 100 cm x 100 cm in plan and 50 cm in height to prepare and test the compacted soil samples (Fig. 3). The selection of these container dimensions was informed by [24] findings, which indicate that the zone of influence for a pile under loading typically extends 3 to 8 pile diameters from the pile axis. Our container size was thus deemed sufficient to mitigate edge effects that could potentially influence the test results. The soil specimen preparation protocol involved compacting the soil in five distinct layers within the container. Compaction was achieved using a manual compaction hammer, a method chosen for its ability to provide consistent and controlled effort across the sample volume. This layered compaction approach was adopted to ensure uniform density distribution throughout the soil mass, which is crucial for obtaining representative and reproducible results in geotechnical testing.

The testing procedure was as the following steps:

- a) Sand density control was achieved by depositing predetermined sand masses into the test container for each layer, followed by surface levelling and compaction to attain the specified relative density.
- b) The initial sand stratum was prepared up to the base level of the model pile base, utilizing a 100 mm thick layer. A minimum 100 mm sand layer was maintained beneath the pile base throughout all experimental tests.
- c) Subsequent sand layers were systematically placed until reaching the designated reinforcement level, whereupon the geogrid was installed on the compacted surface.
- d) The model pile was driven to position at the tank's center using a hammer. The pile was then connected to the loading mechanism via a steel cable system incorporating pulleys and load hanger.
- e) Sand placement continued until achieving the specified fill height ( $Z$ ) above the reinforcement layer.
- f) The loading apparatus was completed by securing the steel cable to the frame-mounted pulleys and positioning the displacement measurement instrumentation.
- g) Loading was implemented incrementally until failure, with each load increment maintained until pile displacement stabilization was achieved.

This soil layer and the geogrid layers represent the case of the single pile reinforced with geogrid, as illustrated in Fig. 4. While Fig. 5 indicates the pile group reinforced with geogrid layers.



**Fig. 3** The metal box (mold) for soil sample preparation.

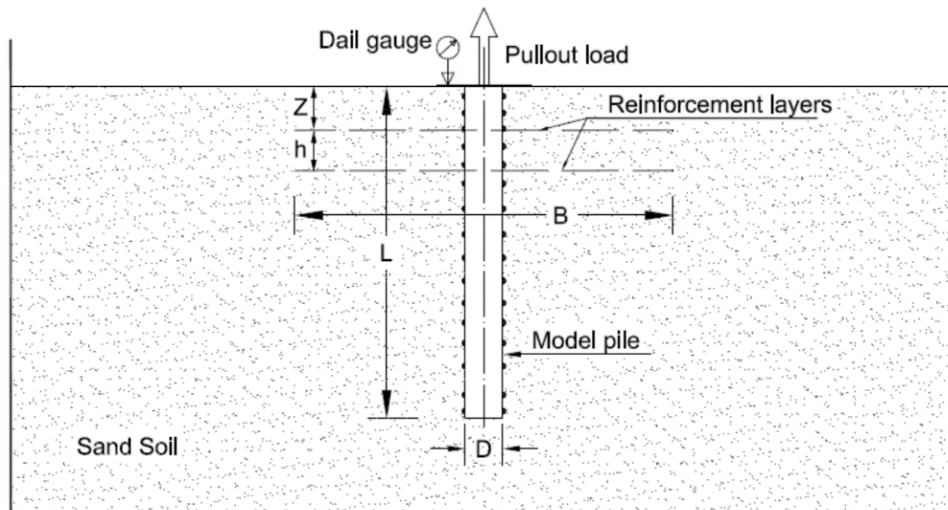


Fig. 4 Single pile reinforced with geogrid.

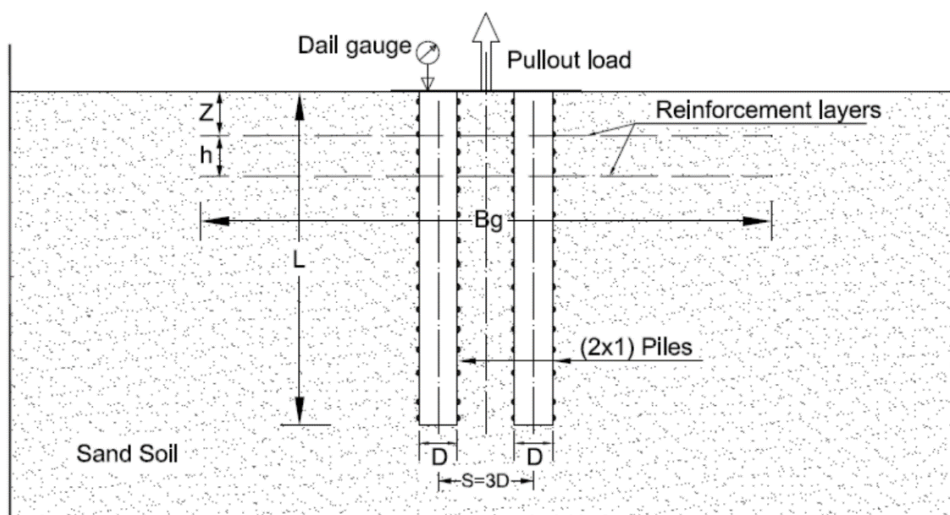


Fig. 5 Pile group reinforced with geogrid.

### 2.3. Experimental Program

A laboratory experiment was carried out on the soil that was previously reported to assess the ability of the single pile or the pile group to resist uplift forces in both unreinforced and reinforced soil conditions. The experimental program aimed to examine the impact of various variables, including the two different types of reinforcement layers, SS30 and TX150. In addition to the reinforcement depth ratio,  $Z/D$ , (depth of reinforcement divided by pile diameter). Also 3 different width ratios of the reinforcement layer for both the single pile and the group of piles,  $B/D$  and  $B_g/D$  (width of reinforcement divided by the pile diameter). Finally, there are two numbers of reinforcement layers ( $N=1$  and  $N=2$ ) were used.

## 2.4. Experimental Results and Analysis

The experiment program mainly includes pullout experiments conducted on a steel pile that is buried in both reinforced and unreinforced soil. Table 2 and Table 3 show the findings of pullout experiments on the single pile and the pile group for the tested soil sample. The load-displacement relationship was analysed to establish optimum load-bearing capacity and corresponding vertical displacement at failure. This point is identified as the peak of the curve or the point where the displacement continues to increase without any further increase in the resistance to pullout. In addition, the efficiency of the pile group ( $\eta$ ) is determined which is the ratio between (the ultimate pullout capacity for the group of piles) to (number of piles\*the ultimate pullout capacity for the single pile).

The findings of the single pile pull-out tests conducted on the soil sample were stated in terms of the improvement ratio (IR). The improvement ratio is calculated by dividing the pullout capacity of reinforced soil by that of unreinforced soil. The IR for each test was determined by dividing the single pullout capacity of reinforced soil ( $T_R$ ) by the single pullout capacity of unreinforced soil ( $T_{un}$ ), expressed as  $IR = T_R/T_{un}$ . Furthermore, the vertical displacement recorded from the pullout tests ( $\Delta h$ ) was documented for all the analysed samples. Additionally, the outcomes of the pile group pull-out tests conducted on the examined soil sample were evaluated using the group improvement ratio (GIR). The group improvement ratio is the ratio of the pullout capacity of a pile group for the reinforced soil to the pullout capacity of a pile group for the unreinforced soil. The GIR (group Improvement Ratio) was determined for each test by dividing the pile group pullout capacity of reinforced soil ( $TR_g$ ) by the pile group pullout capacity of unreinforced soil ( $T_{ung}$ ), expressed as  $GIR = TR_g/T_{ung}$ . Furthermore, the vertical displacement recorded from the pullout tests ( $\Delta h_g$ ) was documented for all the analysed samples. It can be observed in Fig. 6 and Fig. 7 the load-displacement relationship for the single pile reinforced with SS30 and TX150 geogrid. Fig. 8 and Fig. 9 illustrate the load-displacement relationship for the pile group (2x1) that has been reinforced with SS30 and TX150 geogrid.

**Table 2** The findings of the pull-out experiments of the single pile

Test No.	Group	Geogrid Type	(N)	(Z/D)	(h/D)	(B/D)	$T_R$ (kg)	$\Delta h$ (mm)	$IR=T_R/T_{un}$
0	-	No geogrid	-	-	-	-	43	4.97	1.00
1	A	SS30	1	2	-	6	60	2.87	1.40
2						9	64	2.89	1.49
3						12	64	3.55	1.49
4	B		2	2	2	6	85	3.8	1.98
5						9	88	4.08	2.05
6						12	88	3.95	2.05
7	C	TX150	1	2	-	6	55	2.67	1.28
8						9	62	2.37	1.44
9						12	62	2.00	1.44
10	D		2	2	2	6	76	3.62	1.77
11						9	78	2.03	1.81
12						12	78	2.54	1.81

**Table 3** The findings of the pull-out experiments of the pile group

Test No.	Group	Geogrid Type	(N)	(Z/D)	(h/D)	(B/D)	$\frac{(B_g/D)}{(B+S)/D}$	$T_R$ (kg)	$T_{Rg}$ (kg)	$\Delta h_{rg}$ (mm)	$\eta = T_{Rg}/(n*TR)$	$GIR = T_{Rg}/T_{ung}$
0	-	No geogrid	-	-	-	-	-	43	55	4.93	0.64	1.00
1	A	SS30	1	2	-	6	6+3	60	100	3.63	0.83	1.82
2						9	9+3	64	108	3.55	0.84	1.96
3						9	12+3	64	108	4.66	0.84	1.96
4	B		2	2	2	6	6+3	85	115	4.84	0.68	2.09
5						9	9+3	88	119	4.1	0.68	2.16
6						9	12+3	88	119	4.8	0.68	2.16
7	C	TX150	1	2	-	6	6+3	55	90	3.05	0.82	1.64
8						9	9+3	62	100	3.16	0.81	1.82
9						9	12+3	62	100	3.27	0.81	1.82
10	D		2	2	2	6	6+3	76	100	3.5	0.66	1.82
11						9	9+3	78	104	3.24	0.67	1.89
12						9	12+3	78	104	3.33	0.67	1.89

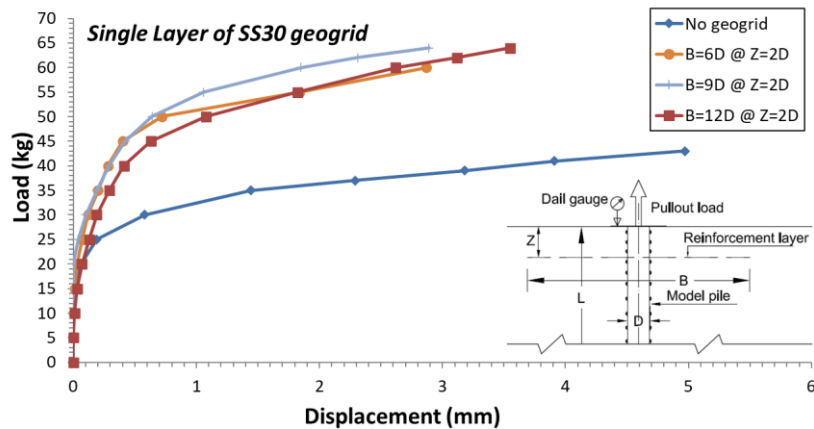


**Fig. 6** Pullout response of single pile in unreinforced soil and reinforced soil for reinforcement type SS30.



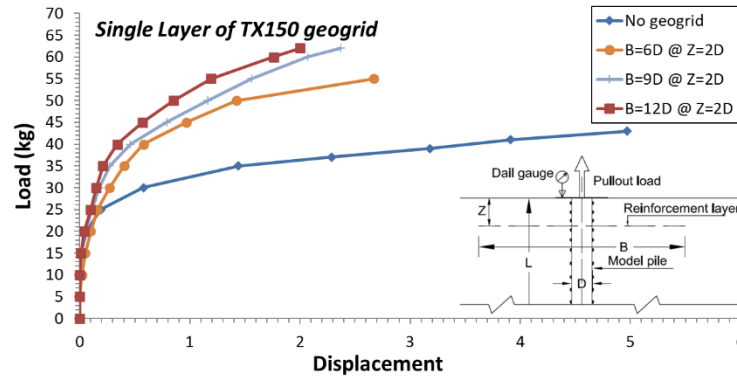


Fig. 7 Pullout response of single pile in unreinforced soil and reinforced soil for reinforcement type TX150.

Fig. 6 and Fig. 7 and Table 2 demonstrate that the pile pullout capacity increases as the reinforcement layers number for the single pile increases. As shown in the table, the maximum IR for the double layers of geogrid it reaches to 2.05 and 1.81 for SS30 and TX150 geogrid, respectively. While for the single layer of geogrid it reaches only to 1.49 and 1.44 for SS30 and TX150 geogrid, respectively. Thus, it can be concluded that utilizing two layers of geogrid with a spacing between the layers of twice the pile diameter is a better and more effective method compared to reinforcing the soil using one layer of geogrid for the single pile.

Additionally, the figures and the table display that the pullout capacity of the pile increases as the reinforcement width ratio (B/D) increases for all tests with a geogrid number of  $N = 1$  and  $N = 2$  up to a B/D ratio of 9 for a single pile. The figures and the table also exhibit that the pile pullout capacity for the SS30 reinforcement type is higher than that of the TX150 reinforcement type. Conversely, the vertical displacement for the TX150 reinforcement type is lower than that of the SS30 reinforcement type.

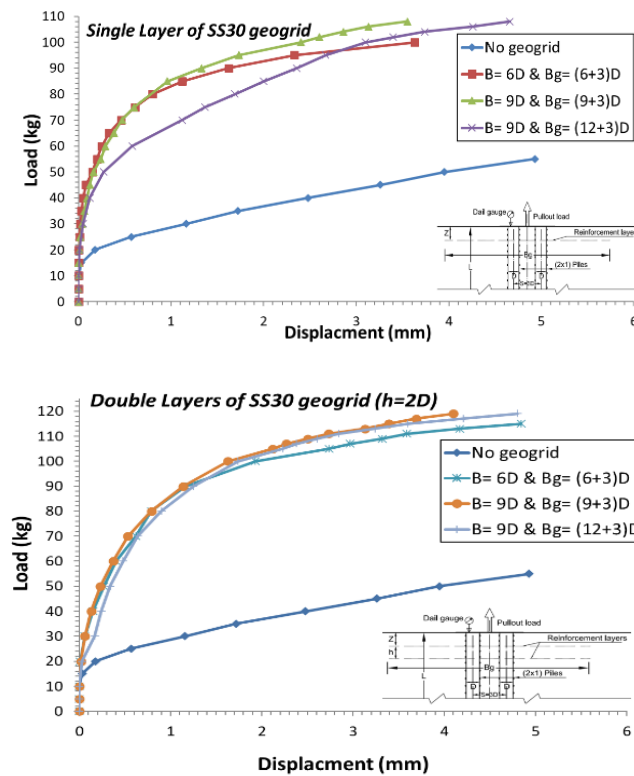
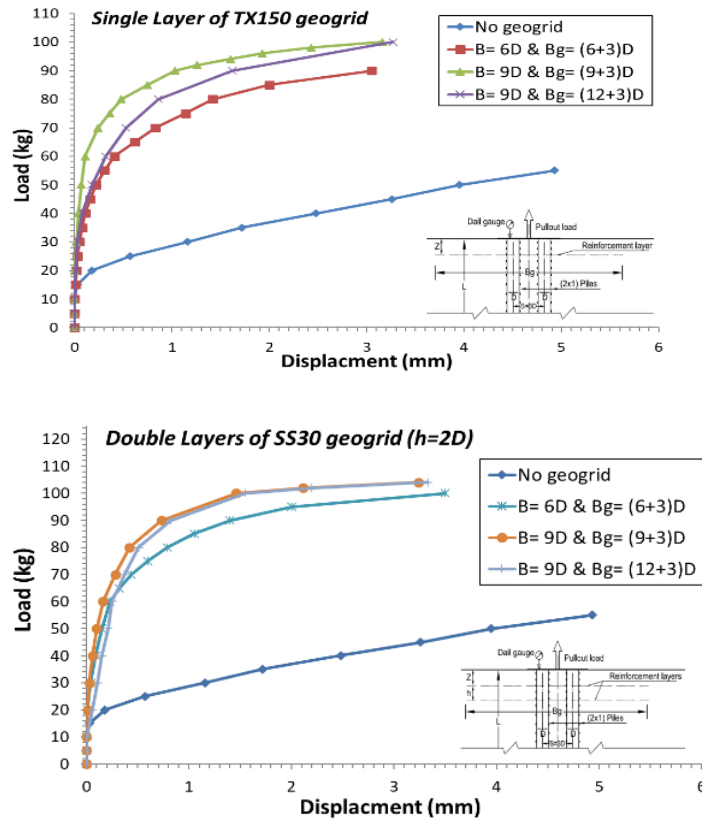


Fig. 8 Pullout response of pile group (2x1) in unreinforced soil and reinforced soil for reinforcement type SS30.



**Fig. 9** Pullout response of pile group (2x1) in unreinforced soil and reinforced soil for reinforcement type TX150.

Fig. 8 and Fig. 9 and Table 3 exhibit that the inclusion of the geogrid layer around group of piles significantly enhances its pullout capacity. Furthermore, using a double layer of geogrid with a distance between the layers that is twice the diameter of the pile will enhance the pile group capacity to a greater extent compared to using one layer of geogrid. As shown in the table, the maximum GIR for the double layers of geogrid it reaches to 2.16 and 1.89 for SS30 and TX150 geogrid, respectively. While for the single layer of geogrid it reaches only to 1.96 and 1.82 for SS30 and TX150 geogrid, respectively. Nevertheless, the group efficiency of one layer of geogrid exceeds that of a double layer of geogrid. Which reaches 0.84 and 0.81 for SS30 and TX150 geogrid of one layer of geogrid, respectively. While, for double layers of geogrid it reaches 0.68 and 0.67 for SS30 and TX150 geogrid, respectively. Thus, it is determined that utilizing one layer of geogrid for the pile group is better and more effective compared to utilizing two layers of geogrid.

Also, the figures and the table demonstrate that the pile group capacity increases as the group reinforcement width ratio ( $B_g/D$ ) increases for all tests with a geogrid number of  $N = 1$  and  $N = 2$  up to a ratio of  $(B_g/D) = (9+3)$  for the pile group. Furthermore, the figures and the table show that the pile group capacity for the SS30 reinforcement type are higher than that of the TX150 reinforcement type. However, the vertical displacement for reinforcement type TX150 is lower than that of the reinforcement type SS30.

### 3. NUMERICAL ANALYSIS

Experimental studies provide an accurate and dependable approach to examining the behaviour of any structure, however more costly than analytical methods and numerical models. Numerical models are suitable for studying and confirming the performance of reinforced pullout piles in geotechnical engineering. Several commercially available finite element programs offer a wide range of applications and produce high-quality outputs. The PLAXIS 2D, PLAXIS 3D, and ABAQUS software packages are widely recognized finite element tools that are commonly employed in diverse geotechnical analytical studies. The finite element analyses (FEA) presented in this study were conducted using the ABAQUS software of Dassault Systems Simula. Creating a 3D full-scale finite element model is advantageous for accurately observing the response of a single pile subjected to vertical pullout loads in non-reinforced and reinforced cohesionless soil. This section presents a thorough set of numerical models that were utilized to assess the efficacy of soil reinforcing in enhancing the resistance of the single piles to pullout loads.

#### 3.1. Numerical Material Properties

The components of the finite element model involve the tested soil materials utilized in this study which is the sandy soil. Furthermore, there are two different kinds of geogrid soil reinforcement that are used to reinforce soils in the constructing of various structures, including road pavements, working platforms, and reinforced foundations. Furthermore, the study utilized a single-pile model to analyze the behaviour of a circular steel pile with bulges.

The soil in the finite element study conducted with ABAQUS was modeled using specifically chosen parameters that accurately represented the geomechanical features of the testing settings. The Mohr-Coulomb model has been utilized to simulate the performance of sand soil. The Mohr-Coulomb model requires the parameters listed in Table 4.

**Table 4:** Mohr-Coulomb parameters utilized for sandy soil in the ABAQUS model

<b>UNITE WEIGHT</b>	18.4 kN/m <sup>3</sup>
<b>YOUNG MODULUS [E]</b>	50000 kN/m <sup>2</sup>
<b>POISSON RATIO [Y]</b>	0.3
<b>FRICTION ANGLE [Φ]</b>	38.3°
<b>DILATANCY ANGLE [Ψ]</b>	8.3°

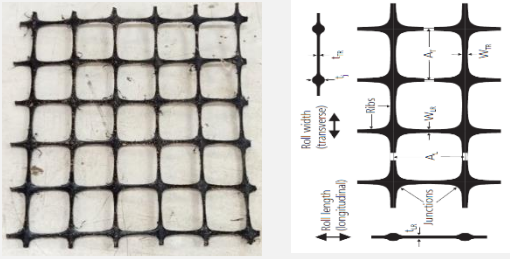
The numerical model effectively represented the behaviour of the pile construction within the soil by incorporating carefully described material qualities and dimensions. The pile was represented as a circular steel pile with bulges, with model pile measurements of 35 mm diameter (D) and 350 mm length (L). The steel pile is represented as a linear elastic material, with steel parameters provided in Table 5.

**Table 5** The ABAQUS pile model parameters

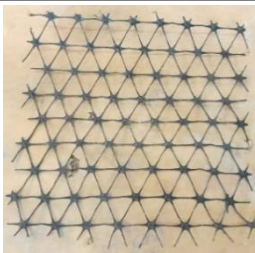
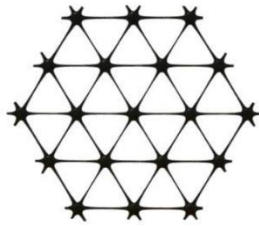
<b>UNITE WEIGHT</b>	78.4 kN/m <sup>3</sup>
<b>YOUNG MODULUS [E]</b>	2E+08 KN/m <sup>2</sup>
<b>POISSON RATIO [Y]</b>	0.3
<b>DIAMETER [D]</b>	35 mm
<b>LENGTH [L]</b>	350 mm

The current study considered the behavior of reinforced layered soil systems using two types of soil reinforcement. The first type of soil reinforcement was a biaxial geogrid of Tensar SS geogrids called (SS30) and the second type of soil reinforcement was a triaxial geogrid of Tensar TriAx geogrids called (TX150). Table 6 and Table 7 show the properties of biaxial SS30 and TriAx geogrids called TX150 geogrid, which were utilized in the present investigation.

**Table 6** Biaxial SS30 geogrid properties utilized for soil reinforcement

<i>Property</i>	<i>Units</i>	<i>SS geogrid Tensar SS30</i>
<i>Polymer</i>		Polypropylene
<i>Minimum carbon black</i>	%	2
<i>Roll width</i>	m	4.0 & 3.8
<i>Roll length</i>	m	50
<i>Unit weight</i>	kg/m <sup>2</sup>	0.33
<i>Roll weight</i>	kg	67 & 64
<b>Dimensions</b>		
<i>AL</i>	mm	39
<i>AT</i>	mm	39
<i>WLR</i>	mm	2.3
<i>WTR</i>	mm	2.8
<i>tJ</i>	mm	5.0
<i>tLR</i>	mm	2.2
<i>tTR</i>	mm	1.3
<i>Biaxial SS30 geogrid used for soil reinforcement</i>		
	<b>control strength longitudinal Quality</b>	
<i>Tult</i>	kN/m	30.0
<i>Load at 2% strain</i>	kN/m	10.5
<i>Load at 5% strain</i>	kN/m	21.0
<i>Approx strain at Tult</i>	%	11.0
<i>Junction strength</i>	%	95
<b>control strength transverse Quality</b>		
<i>Tult</i>	kN/m	30.0
<i>Load at 2% strain</i>	kN/m	10.5
<i>Load at 5% strain</i>	kN/m	21.0
<i>Approx strain at Tult</i>	%	10.0
<i>Junction strength</i>	%	95

**Table 7** Properties of triax geogrids TX150 used for soil reinforcement

Parameter	Longitudinal	Diagonal	Transverse	General	Declared Value	Tolerance
Rib pitch (mm)	40	40	-	-	-	-
Mid-rib depth (mm)	-	1.4	1.1	-	-	-
Mid-rib width (mm)	-	1	1.2	-	-	-
<i>Geogrid opening size (mm)</i>					3	-
Nodal thickness (mm)	-	-	-	-	-	-
Rib shape	-	-	-	rectangular	-	-
Aperture shape	-	-	-	triangular	-	-
Open area aspect (%) ratio	-	-	-	> 85	-	-
<i>TriAx geogrids TX150 used for soil reinforcement</i>						
<i>Tensile strength (KN/m)</i>	-	-	-	-	MD – 20	-4
	-	-	-	-	CMD – 16	-3
<i>Weight (kg/m<sup>2</sup>)</i>	-	-	-	-	0.205	-0.035
<i>Junction efficiency (%)</i>					100	-10
<i>Radial secant stiffness ratio</i>					0.8	-0.15
<i>Radial secant stiffness at 2% strain</i>					250	-65
<i>Radial stiffness at a low strain of 0.5% (kN/m)</i>					360	-75
<i>Where:</i>						
<i>MD: Machine Direction, CMD: Cross- Machin Direction.</i>						

### 3.2. Types of elements and Boundary conditions

The ABAQUS finite element model was carefully constructed to accurately represent the soil-structure system. A total of 5,128 linear hexahedral elements of type C3D8 were used to discretize the domain. The soil component was simulated utilizing a total of 4,968 C3D8 elements. About 160 C3D8 elements were used to model the pile structural component.

The container used in this investigation was full of a 0.45 depth of the soil mass. So, the soil mass was represented as a cylindrical volume with a diameter of 1.0m and a total depth of 0.45m. These dimensions were used to effectively cover the area around the pile that is affected by it, while also minimizing the impact of the boundaries, as illustrated in Fig. 10. In order to improve computational

efficiency while maintaining accuracy, just half of the problem domain was explicitly represented, capitalizing on the axisymmetric characteristics of the pile-soil system. This approach efficiently captures half of the stiffness and loading conditions, resulting in a substantial reduction in solving time without compromising the accuracy of the analysis. The bottom boundary of the soil cylinder was fixed in all directions, while the upper surface was allowed to deform, thereby simulating the conditions of the ground surface. In addition, the sides boundary was an axisymmetric (Y) for symmetric boundary and zero  $U_1$ ,  $U_2$  and  $U_3$  for cylindrical boundary.

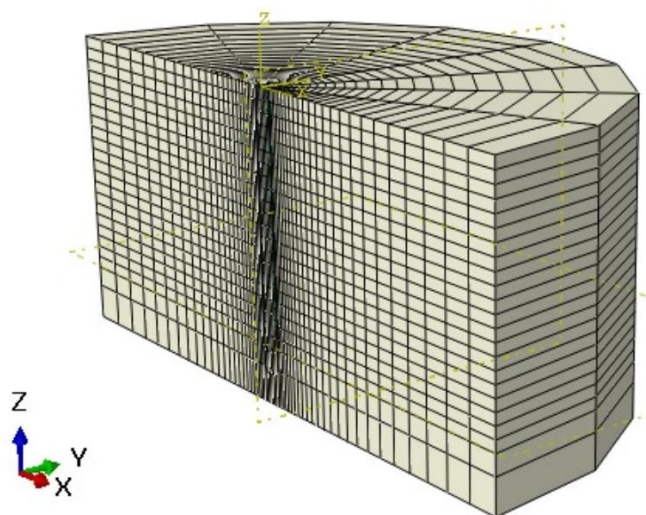


**Fig. 10** The boundary conditions of the numerical model.

### 3.3. Validation of Numerical Results for Single Pile in Unreinforced Soil

The numerical analytical findings are compared to the experimental test results to gain an understanding of the force-displacement behaviour of a single pile in soil without reinforcement. Analyzing the load-displacement relationship yielded the ultimate pullout capacity and the related vertical displacement at failure. Fig. 11 illustrates the differences in load-displacement curves between the experimental and numerical analysis of a single pile in soil without reinforcement. Contours on deformed mesh generated by ABAQUS for a single pile in soil without reinforcement can be seen in Fig. 12.

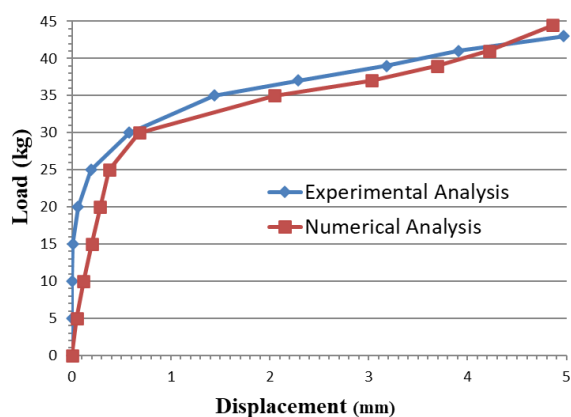


**Fig. 11** Pullout response of the experimental and the numerical analysis of the single pile in unreinforced soil.

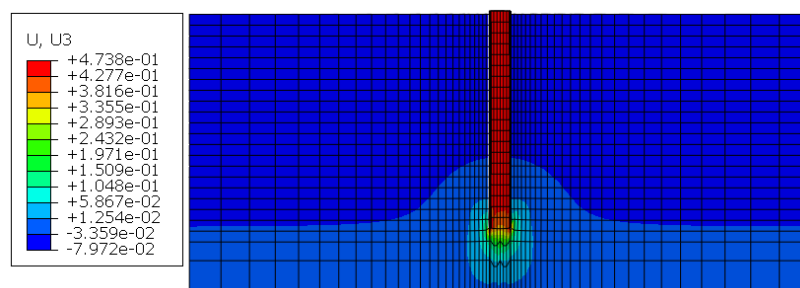


**Fig. 12** Contours on deformed mesh generated by ABAQUS for the single pile in unreinforced soil at the maximum pullout load.

The experimental and numerical simulation findings for single pile in unreinforced soil demonstrate that the variation between the maximum pullout load for the experimental and numerical appears to be about 3.49% (less than 10%), which is excellent. In addition, there is a remarkable congruence, exhibiting consistent trends and outcomes across both methodologies, therefore there is a validating the robustness of our findings and reinforcing our confidence in the applied analytical approaches.

### 3.4. Validation of Numerical Results for Single Pile in Reinforced Soil

The numerical analysis findings are compared to the experimental test data to give an understanding of the force-displacement behaviour of a single pile in reinforced soil. The analysis focuses on one layer of geogrid with a reinforcement width ratio ( $B/D$ ) of 6 and a reinforcement depth ratio ( $Z/D$ ) of 2. Analyzing the load-displacement relationship yielded the ultimate pullout capacity and the related vertical displacement at failure. Fig. 13 illustrates the load-displacement curves for both the experimental and numerical analysis of a single pile in reinforced soil using geogrid type SS30. Furthermore, Fig. 14 illustrates the load-displacement curves for both the experimental and numerical analysis of a single pile in reinforced soil using geogrid type TX150. Contours on deformed mesh generated by ABAQUS for a single pile in reinforcement soil can be seen in Fig. 15.

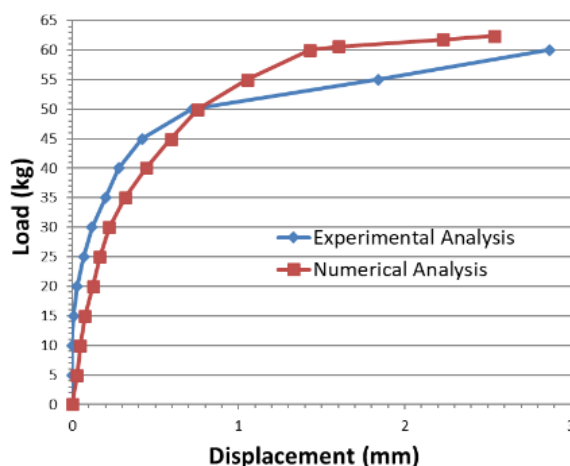


**Fig. 13** Pullout response of the experimental and the numerical analysis of the single pile in reinforced soil of geogrid type (SS30).

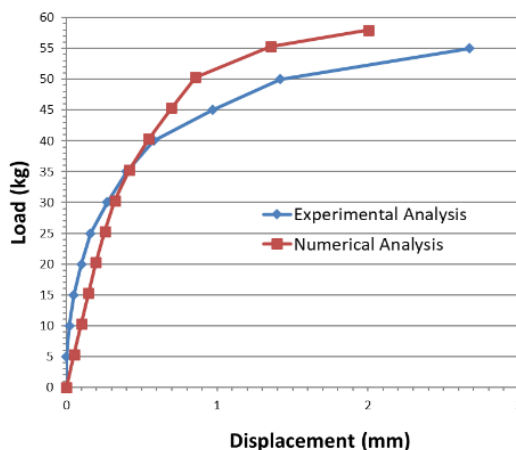


**Fig. 14** Pullout response of the experimental and the numerical analysis of the single pile in reinforced soil of geogrid type (TX150).

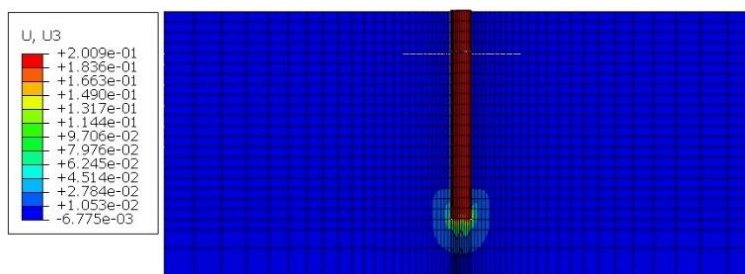


**Fig. 15** Contours on deformed mesh generated by ABAQUS for the single pile in TX150 reinforced soil at the maximum pullout load.

The experimental and numerical simulation findings for single pile in reinforced soil demonstrate that the variation between the maximum pullout load for the experimental and numerical appears to be about 4.1% and 5.45% for the reinforced type SS30 and TX150, respectively (less than 10%), which is excellent. In addition, there is a remarkable congruence, exhibiting consistent trends and outcomes across both methodologies, therefore there is a validating the robustness of our findings and reinforcing our confidence in the applied analytical approaches.

#### 4. CONCLUSIONS

The present investigation was carried out experimentally and numerically to assess the influence of soil reinforcement on the performance of single pile under pullout loads. Relationships to assess the single pile pullout capacity and the group pullout capacity for reinforcement types (SS30) and (TX150) by varying the parameters such as the single pile reinforcement width ratio ( $B/D$ ), the pile group reinforcement width ratio ( $B_g/D$ ) and the reinforcement layer number ( $N$ ) were established from the obtained results of the considered tested soil. Nevertheless, once all laboratory results were combined, acceptable relationships were revealed. The findings from the present investigation may be summarised as follows:

- a) For the single pile:
  1. The inclusion of a geogrid layer around pile significantly increases its pullout capacity.
  2. The optimum reinforcement width ratio ( $B/D$ ) is considered to be approximately equal to 9.0 times the pile diameter.



3. There is an increase in the pullout capacity for the reinforcement type SS30 than the reinforcement type TX150. In addition, there is a decrease in the vertical displacement ( $\Delta h$ ) for the reinforcement type TX150 than the reinforcement type SS30.
  4. The experimental and numerical simulation results demonstrate remarkable congruence, exhibiting consistent trends and outcomes across both methodologies, therefore there is a validating the robustness of our findings and reinforcing our confidence in the applied analytical approaches.
- b) For the pile group:
1. The inclusion of a geogrid layer around the pile group significantly increases its pullout capacity. However, the group efficiency of the single layer of geogrid is more than the group efficiency of a double layer of geogrid. Therefore, for the pile group it is concluded that using one layer of geogrid is better and more effective than reinforcing the soil itself with double layers of geogrid.
  2. The optimum reinforcement width ratio ( $B_g/D$ ) is considered to be approximately equal to  $(9+3)$  times the pile diameter.
  3. There is an increase in the group pullout capacity for the reinforcement type SS30 than the reinforcement type TX150. In addition, there is a decrease in the vertical displacement ( $\Delta h_{Rg}$ ) for the reinforcement type TX150 than the reinforcement type SS30.
  4. The group efficiency ( $\eta$ ) improved by adding one reinforcement layer (0.84 and 0.81 for SS30 and TX150 geogrid) rather than two layers (0.68 and 0.67 for SS30 and TX150 geogrid).

## References

- [1] A. T. Ghalesari and H. Rasouli, "Effect of Gravel Layer on the Behavior of Piled Raft Foundations," pp. 373–382, May 2014, doi: 10.1061/9780784413425.038.
- [2] A. Taghavi Ghalesari, A. Barari, P. Fardad Amini, and L. B. Ibsen, "Development of optimum design from static response of pile–raft interaction," *Journal of Marine Science and Technology (Japan)*, vol. 20, no. 2, pp. 331–343, Jun. 2015, doi: 10.1007/S00773-014-0286-X/FIGURES/15.
- [3] M. Modarresi, H. Rasouli, A. T. Ghalesari, and M. H. Baziar, "Experimental and Numerical Study of Pile-to-Pile Interaction Factor in Sandy Soil," *Procedia Eng*, vol. 161, pp. 1030–1036, Jan. 2016, doi: 10.1016/J.PROENG.2016.08.844.
- [4] A. Barari, L. B. Ibsen, A. Taghavi Ghalesari, and K. A. Larsen, "Embedment Effects on Vertical Bearing Capacity of Offshore Bucket Foundations on Cohesionless Soil," *International Journal of Geomechanics*, vol. 17, no. 4, p. 04016110, Apr. 2017, doi: 10.1061/(ASCE)GM.1943-5622.0000782.
- [5] A. Taghavi Ghalesari and A. Janalizadeh Choobbasti, "Numerical analysis of settlement and bearing behaviour of piled raft in Babol clay," *European Journal of Environmental and Civil Engineering*, vol. 22, no. 8, pp. 978–1003, Aug. 2018, doi: 10.1080/19648189.2016.1229230.
- [6] A. K. Choudhary, J. N. Jha, and K. S. Gill, "Laboratory investigation of bearing capacity behaviour of strip footing on reinforced flyash slope," *Geotextiles and Geomembranes*, vol. 28, no. 4, pp. 393–402, Aug. 2010, doi: 10.1016/J.GEOTEXMEM.2009.09.007.

- [7] M. El Sawwaf and A. Nazir, "Behavior of Eccentrically Loaded Small-Scale Ring Footings Resting on Reinforced Layered Soil," *Journal of Geotechnical and Geoenvironmental Engineering*, vol. 138, no. 3, pp. 376–384, Jun. 2012, doi: 10.1061/(ASCE)GT.1943-5606.0000593.
- [8] B. Leshchinsky and H. I. Ling, "Numerical modeling of behavior of railway ballasted structure with geocell confinement," *Geotextiles and Geomembranes*, vol. 36, pp. 33–43, Feb. 2013, doi: 10.1016/J.GEOTEXMEM.2012.10.006.
- [9] H. I. Ling and H. Liu, "Deformation analysis of reinforced soil retaining walls-simplistic versus sophisticated finite element analyses," *Acta Geotech*, vol. 4, no. 3, pp. 203–213, Jul. 2009, doi: 10.1007/S11440-009-0091-6/FIGURES/10.
- [10] J. Lovisa, S. K. Shukla, and N. Sivakugan, "Behaviour of prestressed geotextile-reinforced sand bed supporting a loaded circular footing," *Geotextiles and Geomembranes*, vol. 28, no. 1, pp. 23–32, Feb. 2010, doi: 10.1016/J.GEOTEXMEM.2009.09.002.
- [11] G. M. Latha and A. Somwanshi, "Bearing capacity of square footings on geosynthetic reinforced sand," *Geotextiles and Geomembranes*, vol. 27, no. 4, pp. 281–294, Aug. 2009, doi: 10.1016/J.GEOTEXMEM.2009.02.001.
- [12] S. N. M. Tafreshi, O. Khalaj, and M. Halvae, "Experimental study of a shallow strip footing on geogrid-reinforced sand bed above a void," <https://doi.org/10.1680/gein.2011.18.4.178>, vol. 18, no. 4, pp. 178–195, May 2011, doi: 10.1680/GEIN.2011.18.4.178.
- [13] B. F. Tanyu, A. H. Aydilek, A. W. Lau, T. B. Edil, and C. H. Benson, "Laboratory evaluation of geocell-reinforced gravel subbase over poor subgrades," <https://doi.org/10.1680/gein.13.00001>, vol. 20, no. 2, pp. 47–61, May 2013, doi: 10.1680/GEIN.13.00001.
- [14] X. Yang, J. Han, D. Leshchinsky, and R. L. Parsons, "A three-dimensional mechanistic-empirical model for geocell-reinforced unpaved roads," *Acta Geotech*, vol. 8, no. 2, pp. 201–213, Apr. 2013, doi: 10.1007/S11440-012-0183-6/FIGURES/11.
- [15] N. C. Consoli, C. A. Ruvier, V. Girardello, L. Festugato, and A. Thomé, "Effect of polypropylene fibers on the uplift behavior of model footings embedded in sand," <https://doi.org/10.1680/gein.2012.19.1.79>, vol. 19, no. 1, pp. 79–84, May 2012, doi: 10.1680/GEIN.2012.19.1.79.
- [16] M. El Sawwaf and A. Nazir, "The effect of soil reinforcement on pullout resistance of an existing vertical anchor plate in sand," *Comput Geotech*, vol. 33, no. 3, pp. 167–176, Apr. 2006, doi: 10.1016/J.COMPGeo.2006.04.001.
- [17] A. Ghosh and A. K. Bera, "Effect of Geotextile Ties on Uplift Capacity of Anchors Embedded in Sand," *Geotechnical and Geological Engineering*, vol. 28, no. 5, pp. 567–577, Mar. 2010, doi: 10.1007/S10706-010-9313-9/TABLES/6.
- [18] K. Ilamparuthi and E. A. Dickin, "Predictions of the uplift response of model belled piles in geogrid-cell-reinforced sand," *Geotextiles and Geomembranes*, vol. 19, no. 2, pp. 89–109, Mar. 2001, doi: 10.1016/S0266-1144(00)00011-X.
- [19] K. Ilamparuthi and E. A. Dickin, "The influence of soil reinforcement on the uplift behaviour of belled piles embedded in sand," *Geotextiles and Geomembranes*, vol. 19, no. 1, pp. 1–22, Jan. 2001, doi: 10.1016/S0266-1144(00)00010-8.

- [20] S. V. K. Rao and A. M. Nasr, "Behavior of vertical piles embedded in reinforced sand under pullout oblique loads," *International Journal of Geotechnical Engineering*, vol. 4, no. 2, pp. 217–230, Apr. 2010, doi: 10.3328/IJGE.2010.04.02.217-230.
- [21] B. Li and J. Fu, "Analysis of uplift bearing capacity of pile based on ABAQUS," *IOP Conf Ser Earth Environ Sci*, vol. 61, no. 1, p. 012097, Apr. 2017, doi: 10.1088/1755-1315/61/1/012097.
- [22] J. Jiang, Z. Mao, L. Chen, and Y. Wu, "Finite Element Analysis of Load-Bearing Characteristics and Design Method for New Composite-Anchor Uplift Piles," *Applied Sciences 2024, Vol. 14, Page 2100*, vol. 14, no. 5, p. 2100, Mar. 2024, doi: 10.3390/APP14052100.
- [23] B. K. Mazurkiewicz, "SKIN FRICTION ON MODEL PILES IN SAND," 1968.
- [24] A. K. Verma and R. K. Joshi, "Uplift Load Carrying Capacity of Piles in Sand," *Indian Geotechnical Conference – 2010, GEOTrendz, IGS Mumbai Chapter & IIT Bombay*, 2010.